Lithium and Beryllium in One-solar-mass Stars

Ann Merchant Boesgaard[1,4] , Constantine P. Deliyannis[2,4] , Michael G. Lum[1,4] , and Ashley Chontos[1,3,4]

[1] Institute for Astronomy, University of Hawai'i at Manoa, 2680 Woodlawn Drive, Honolulu, HI 96822, USA; annmb@hawaii.edu, mikelum@mac.com
[2] Department of Astronomy, Indiana University, 727 East 3rd Street, Swain Hall West 319, Bloomington, IN 47405–7105, USA; cdeliyan@indiana.edu
[3] Astrophysical Sciences, Peyton Hall, Princeton, NJ 08544, USA; ashleychontos@princeton.edu

Abstract

The surface content of lithium (Li) and beryllium (Be) in stars can reveal important information about the temperature structure and physical processes in their interior regions. This study focuses on solar-type stars with a sample that is more precisely defined than done previously. Our selection of stars studied for Be is constrained by five parameters: mass, temperature, surface gravity, metallicity, and age to be similar to the Sun and is focused on stars within ± 0.02 of $1\,M_\odot$. We have used the Keck I telescope with HIRES to obtain spectra of the Be II spectral region of 52 such stars at a high spectral resolution ($\sim$45,000) and high signal-to-noise ratios. While the spread in Li in these stars is greater than a factor of 400, the spread in Be is only 2.7 times. Two stars were without any Be, perhaps due to a merger or a mass transfer with a companion. We find a steep trend of Li with temperature but little for Be. While there is a downward trend in Li with [Fe/H] from -0.4 to $+0.4$ due to stellar depletion, there is a small increase in Be with Fe from Galactic Be enrichment. While there is a broad decline in Li with age, there may be a small increase in Be with age, though age is less well determined. In the subset of stars closest to the Sun in temperature and other parameters, we find that the ratio of the abundances of Be to Li is much lower than predicted by models; there may be other mixing mechanisms causing additional Li depletion.

Unified Astronomy Thesaurus concepts: Stellar abundances (1577); Stellar atmospheres (1584); Stellar astronomy (1583); Stellar interiors (1606)

1. Introduction

In 1951, Greenstein & Richardson (1951) showed that Li in the Sun was only one-hundredth as abundant as on Earth. They speculated that if material containing Li were circulated to temperatures near 3×10^6 K, the Li nuclei would be lost by thermonuclear disintegration. They suggested that any mixing of the surface material with regions of such temperatures would have to be very slow for there to be any surface Li at all. The most recent assessment of solar Li is $A(\mathrm{Li}) = 0.96 \pm 0.06$, where $A(\mathrm{Li}) = \log N(\mathrm{Li}) - \log N(\mathrm{H}) + 12.00$ (Asplund et al. 2021). The solar system Li content is $A(\mathrm{Li}) = 3.27 \pm 0.03$ (Lodders 2021) or about 200 times greater.

By 1954, Greenstein & Tandberg Hansen (1954) have measured the abundance of Be in the Sun from lines of both Be II and Be I and found it to be similar to the Be content in meteorites and on Earth. They knew then that the Sun had not destroyed its Be and thus Be nuclei would not have been transported to temperatures of 3.6×10^6 K. The current evaluation of solar Be is $A(\mathrm{Be}) = 1.38 \pm 0.09$ (Asplund et al. 2021) and that of meteoritic Be is 1.31 ± 0.04 (Lodders 2021), where $A(\mathrm{Be}) = \log N(\mathrm{Be}) - \log N(\mathrm{H}) + 12.00$.

The solar Li abundance is observed to be down by more than 200 compared to the solar system value while the solar and meteoritic Be abundances are comparable to each other. The Standard Stellar Evolution Theory (SSET) has been unable to account for this low value of solar Li while recognizing that

any main-sequence mixing processes had to be slow and involve additional mixing mechanisms. Somers & Pinsonneault (2016) discuss Li depletion with a modification in the role of differential rotation. They include more angular momentum transport and determine that core-envelope recoupling produces efficient mixing.

In order to understand solar Li depletion, several studies have been done on Li in solar twins, e.g., Matsuno et al. (2017) and Thevenin et al. (2017). A recent example is that of Carlos et al. (2019), who determined Li abundances in 77 solar "twins." They conclude that the Sun "is unusually Li-deficient for it is age." They define twins by temperature (± 100 K), $\log g$ (± 0.01), and [Fe/H] (± 0.01), approximately. Their sample does not constrain mass or age, but 30 stars are within $\pm 2\%$ of the solar mass, and of those, 16 are within 2 billion years of the age of the Sun. For those 16, their values for LTE Li range from 0.91 to 1.76 plus one with an upper limit of <0.49. The Sun at 0.96 is close to the bottom of the range.

Boesgaard et al. (2020) studied Li and Be in the solar-age and solar-metallicity open cluster M67. In their Figures 7 and 8, they indicated the position of the solar Li value. In both figures of Li versus temperature and Li versus mass, the Sun is in the lower third of the range of Li in M67, but not particularly out of line in the Li trends.

Although it is much more difficult to make observations of Be than Li, its abundance is an important ingredient to our understanding of stellar interiors. Both Li and Be are destroyed primarily by energetic protons but whereas Li survives to a depth where T is $\sim 2.5 \times 10^6$ K, Be nuclei survive deeper in the star to $\sim 3.5 \times 10^6$ K. Abundances of both elements, therefore, produce information about the interiors and the processes at work that affect their depletion.

There have been some previous attempts to find Be in solar-like stars with known Li. Boesgaard & Hollek (2009) found Be

Table 1
Log of the Keck/HIRES Be Observations in Solar-mass Stars

HIP	HD	V	Date (UT)	Exp. (minutes)	S/N
394	225239	6.10	2014 Dec 26	2	102
493	101	7.45	2014 Dec 26	5	93
996	804	8.18	2014 Jan 15	5	71
1411	1327	9.06	2014 Jan 15	15	65
1813	1832	8.3	2019 Dec 03	10	156
7244	9472	7.63	2014 Dec 27	7	96
7245	9446	8.35	2014 Jan 15	7	85
23627	32724	7.20	2014 Jan 15	5	82
24813	34411	4.71	2017 Nov 10	1	154
25002	35041	7.68	2017 Nov 10	4	79
25052	34634	7.74	2017 Nov 11	7	76
25414	35073	8.34	2014 Jan 15	7	44
30860	45350	7.88	2014 Jan 15	6	91
31965	47309	7.60	2017 Nov 11	10	72
32673	49178	8.07	2014 Jan 15	7	98
35599	56196	8.96	2014 Jan 15	17	38
41184	70516	7.70	2017 Nov 11	6	80
42438	72905	5.65	2014 Jan 15	5	32
42723	74156	7.61	2017 Nov 10	5	108
44935	78534	8.71	2014 Jan 15	20	48
49580	87680	7.98	2014 Dec 28	10	87
50473	80307	7.03	2014 Dec 27	4	106
52153	92242	8.34	2014 Dec 28	11	90
54196	96094	7.62	2014 Dec 28	10	104
54582	97037	6.81	2014 Dec 27	4	96
55846	99491	6.49	2014 Dec 28	3	85
56572	100777	8.42	2014 Jan 15	8	60
57300	102081	8.27	2014 Dec 28	10	110
58576	104304	5.54	2014 Dec 27	1	78
62039	110537	7.83	2014 Dec 27	5	77
62198	110835	9.06	2014 Jan 15	10	68
63354	112756	8.13	2014 Dec 27	5	84
65049	115968	8.02	2014 Jan 15	5	72
65708	117126	7.44	2014 Dec 27	5	82
72567	130948	5.88	2014 Jan 15	3	189
73146	132406	8.45	2014 Jan 15	10	56
100017	193664	5.93	2017 Nov 11	2	73
100963	195034	7.09	2017 Nov 11	3	86
100970	195019	6.97	2017 Nov 11	3	95
104075	200746	7.99	2019 Dec 03	6	59
106678	205656	8.61	2019 Dec 04	10	86
107350	206860	5.95	2017 Nov 10	3	170
108468	208704	7.17	2017 Nov 10	3	52
109090	209858	7.79	2017 Nov 10	5	122
109110	209799	7.58	2017 Nov 10	5	84
109378	210277	6.63	2017 Nov 10	5	155
109931	24°4563	8.95	2017 Nov 11	10	74
110035	211476	7.04	2019 Dec 03	6	54
112504	215696	7.33	2017 Nov 10	3	47
115370	220255	7.77	2017 Nov 11	6	108
116906	222582	7.69	2017 Nov 11	6	50
118115	224383	7.88	2017 Nov 11	8	48
118159	224448	9.01	2017 Nov 11	12	77

Table 2
Stellar Parameters for the Solar-mass Stars

HIP	$T_{\rm eff}$ (K)	log g	[Fe/H]	ξ	A(Li)	Mass	Age (Gyr)
394	5636	3.76	−0.49	1.92	1.98	1.10	5.00
493	5943	4.38	−0.23	1.36	2.31	0.99	5.77
996	5817	4.32	−0.04	1.34	1.45	1.00	6.83
1411	5788	4.45	−0.03	1.14	1.27	0.99	4.84
1813	5756	4.30	−0.03	1.32	<1.08	0.98	7.95
7244	5767	4.46	−0.07	1.12	2.26	0.99	4.38
7245	5801	4.42	+0.08	1.20	1.82	1.02	3.45
23627	5791	4.15	−0.19	1.54	1.57	1.00	9.79
24813	5860	4.23	+0.05	1.48	2.03	1.05	6.55
25002	5741	4.44	−0.11	1.12	2.36	0.95	6.51
25052	5749	4.24	+0.09	1.39	<0.34	1.03	8.27
25414	5647	4.46	+0.07	0.98	<1.13	0.98	5.09
30860	5527	4.18	+0.25	1.29	<0.14	1.01	10.52
31965	5782	4.33	+0.02	1.30	0.96	1.01	7.30
32673	5736	4.44	+0.03	1.12	<1.07	0.99	6.61
35599	5820	4.19	−0.10	1.51	1.63	1.01	8.40
41184	5717	4.41	+0.08	1.14	2.85	0.99	4.79
42438	5876	4.49	−0.07	1.16	2.94	1.01	0.20
42723	6018	4.11	+0.04	1.77	2.52	1.17	5.35
44935	5759	4.33	+0.04	1.28	<0.88	1.00	7.60
49580	5794	4.51	−0.01	1.07	1.95	1.00	1.69
50473	5925	4.34	−0.17	1.40	2.20	1.00	6.64
52153	5791	4.15	−0.17	1.59	1.91	0.99	8.96
54196	5877	4.09	−0.35	1.68	2.51	0.99	8.72
54582	5826	4.22	−0.12	1.48	1.56	1.00	9.26
55846	5463	4.48	+0.30	0.85	0.96	0.99	3.45
56572	5511	4.39	+0.30	1.00	<0.37	0.99	6.43
57300	6064	4.19	−0.35	1.70	2.42	1.02	6.50
58576	5508	4.42	+0.31	0.96	0.32	1.00	6.71
62039	5658	4.34	+0.11	1.18	0.72	0.99	8.99
62198	5712	4.34	+0.07	1.23	1.05	1.00	8.67
63354	6066	4.40	−0.34	1.43	2.55	1.00	5.04
65049	5539	4.25	+0.20	1.21	<0.66	0.99	10.95
65708	5735	4.17	−0.07	1.47	0.69	1.00	9.93
72567	5942	4.39	−0.11	1.35	2.86	1.00	0.60
73146	5731	4.22	+0.07	1.40	1.22	1.02	8.78
100017	5902	4.42	−0.14	1.28	2.22	1.01	4.81
100963	5786	4.44	−0.03	1.16	1.63	0.99	5.66
100970	5733	4.09	+0.04	1.57	1.29	1.06	8.63
104075	5893	4.36	+0.02	1.35	2.71	1.04	0.40
106678	5644	4.14	+0.01	1.43	0.42	0.99	10.14
107350	5942	4.45	−0.08	1.14	2.93	1.03	0.20
108468	5799	4.34	−0.11	1.30	<1.03	0.98	7.81
109090	5993	4.23	−0.24	1.60	2.41	1.03	7.46
109110	5815	4.46	+0.03	1.15	2.45	1.03	0.70
109378	5526	4.38	+0.22	1.03	<0.41	0.98	9.91
109931	5734	4.34	+0.04	1.24	0.82	0.98	6.71
110035	5830	4.35	−0.19	1.31	1.65	0.95	8.79
112504	5753	4.36	−0.02	1.23	1.97	0.98	6.82
115370	5896	4.29	−0.02	1.44	1.85	1.05	6.79
116906	5744	4.31	−0.01	1.29	1.08	0.99	8.51
118115	5836	4.32	+0.00	1.36	<1.11	1.02	6.87
118159	5848	4.42	−0.05	1.23	2.71	1.02	5.77

in 50 "solar-mass" stars, although their sample ranged in mass from 0.90 to 1.09 $M_\odot$. Most of their stars were below [Fe/H] = −0.15 and the Be abundances in the thin-disk stars fit well with the Be–Fe trend found for halo metal-poor stars found by Boesgaard et al. (2011); that relationship was shown to extend over 4 orders of magnitude in [Fe/H] and 3 orders of magnitude in A(Be) as shown in their Figure 11. Four stars in their sample, all subgiants, showed strong depletions of Be.

Takeda et al. (2011) determined Be abundance in 118 solar "analogs" but had an even larger range in parameters with [Fe/H] from −0.6 to +0.4 and temperatures from 5000 to 7000 K, but centered on 5775 K, and masses of 0.8–1.7 $M_\odot$. They found little dependence of A(Be) on metallicity, temperature, or age in the early G stars, but a small increase with $v \sin i$ between 1 and 7 km s^{-1}. In their sample, there were four stars that were severely deficient in Be and Li.
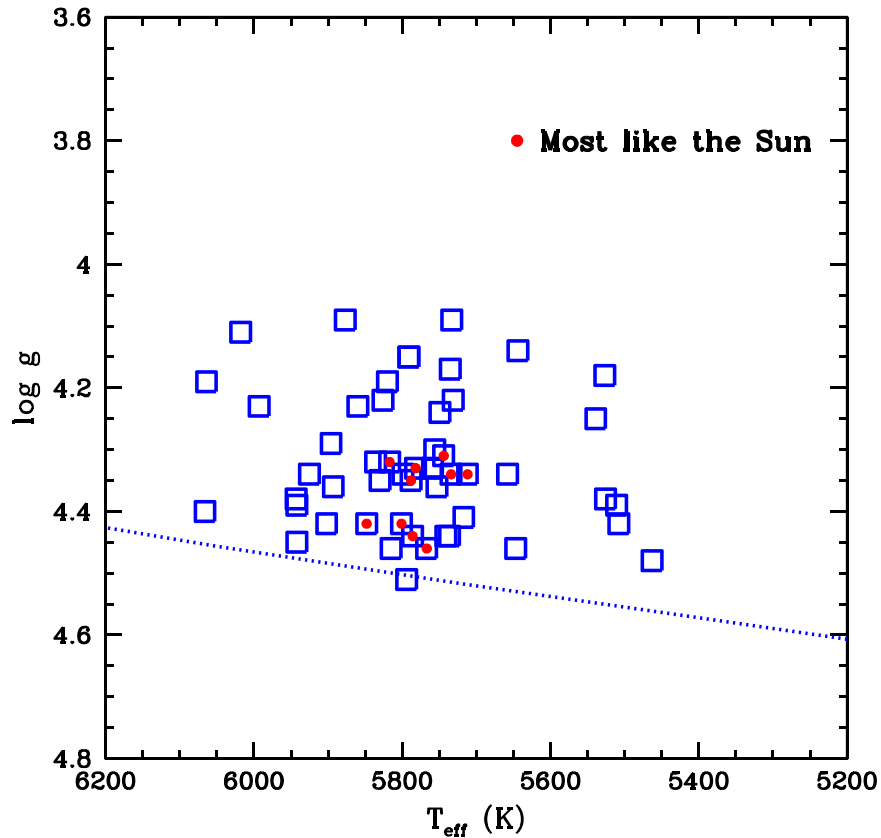
Figure 1. The distribution of the stars we observed by their surface temperatures and gravities as log *g* from Ramirez et al. (2012), shown as blue open squares. The zero-age main sequence is indicated by the dotted line from Demarque et al. (2004). The 10 stars that are closest to the Sun in all five parameters have small red dots inside the open squares.

Chmielewski et al. (1975) did a careful examination of the solar Be amount and found $A(Be) = 1.15 \pm 0.20$. This value is lower by almost a factor of 2 than the meteoritic value of 1.42 (Anders & Grevesse 1989). Balachandran & Bell (1998) suggest this deficiency is not real but is due to missing *uv* opacity or differences between the predicted and observed solar *uv* flux. However, as mentioned above, recent compilations of solar and solar system abundances show better agreement for Be. Asplund et al. (2021) found $A(Be) = 1.38 \pm 0.09$ for the Sun. For meteorites, Lodders (2021) gives $A(Be) = 1.31 \pm 0.04$.

In this work, we take another observational approach to understand Li and Be in stars and to help clarify the solar Li and Be issues. The sample presented in this paper is more restrictive than those done previously. It has a narrower range in mass, temperature, and [Fe/H]. All of our targets are from a collection of 1581 FGK stars with a consistent set of stellar parameters and Li abundances by Ramirez et al. (2012). They have determined and cataloged their Li abundances, ages, effective temperatures, surface gravities, masses, and metallicities along with the associated errors in those determinations. They also indicate whether each star belongs to the thin-disk, thick-disk, or halo population. From their list, we have selected stars to observe for Be that are predominantly within $\pm 2\%$ of $1\,M_\odot$.

2. Observations and Stellar Parameters

We have observed Be in stars of $1\,M_\odot$ selected from the sample of 1381 FGK stars for which Ramirez et al. (2012)

determined Li abundances. Their sample includes Li abundances in 671 newly observed stars supplemented by 710 Li determinations by others normalized to their scale. They give the offsets they used for each of the seven other studies they included in their Table 2. For all of the stars, they give errors in the stellar parameters. For the solar-mass stars we have observed, the errors in the mass determinations are given as $+0.02, -0.03$ or $+0.03, -0.02$. (Two of our stars, HIP 394 and HIP 42723, are out of our mass range and error range at $1.10 + 0.15, -0.05$ and $1.17 + 0.17$, respectively.) All of our sample of stars are from the thin disk, except HIP 35599, which is from the thick disk. One star is a subgiant, HIP 394.

Our Be spectra were obtained with HIRES (Vogt et al. 1994) on the Keck I telescope with the upgraded version (2004)[5] during the course of four observing runs between 2014 January and 2019 December. The spectrograph has three CCD chips, and our wavelength coverage was from 3035–5880 Å. The Be II resonance lines are at 3130.42 and 3131.06 Å on the blue chip near the atmospheric cutoff of ~3000 Å. This blue CCD has a quantum efficiency of 94% at 3130 Å so we could observe our stars with short exposure times yet high signal-to-noise ratios (S/N). The spectral resolution was ~45,000 or 0.023 Å per pixel.

For our sample of 53 solar-mass stars, the exposures ranged from 1–20 minutes with most being less than 10 minutes. The values of S/N near the Be II lines ranged from 50 to 190, with most between 70 and 100. The stars were bright with only six having *V* magnitudes fainter than 8.5. In order to minimize the
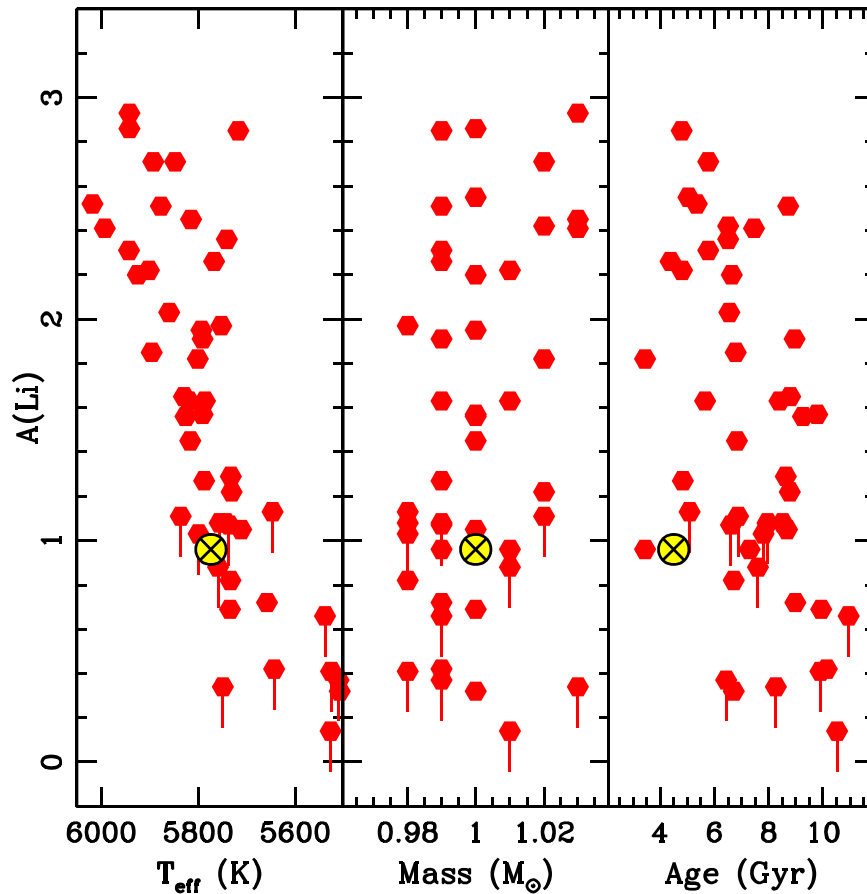
---

[5] https://www.ucolick.org/~vogt/hires.html

Figure 2. Abundances of Li as A(Li) in the solar-mass stars we have observed for Be shown as functions of surface temperature, stellar mass, and age. The values are from Ramirez et al. (2012). The position of the Sun is the yellow circled X at A(Li) = 0.96 (Asplund et al. 2021). The vertical lines attached to some of the Li points indicate that those Li values are upper limits. The mass range is very close to solar, within ± 0.02. The solar temperature is 5772 K; most of our stars are within ± 100 K of that. The age of the Sun is 4.60 Gyr; 75% of our stars are within a factor of 2 of that age.

effects of atmospheric attenuation and refraction, we observed the stars as close to the meridian as possible. Our candidate list was long enough to make this straightforward.

During each night of observing, we obtained 1 s exposures of a Th–Ar comparison spectrum at the beginning and end of the night for wavelength calibration. Several exposures were taken of a quartz lamp to enable the flat-fielding of the science frames. These exposures for the blue CCD had to be 45 s to get enough signal near 3130 Å. Typically 11 bias frames of 0^s were taken for background corrections. The data reduction process was enabled by the MAKEE pipeline.[6] The Th–Ar spectra turned out to be identical at the beginning and end of the night and were used to make the preliminary wavelength adjustments; the final wavelength corrections were done with IRAF (Tody 1986, 1993).[7] We have on hand a Keck/HIRES spectrum taken of the daytime sky at sunrise to use as a surrogate for the solar spectrum in the Be II spectral region. That exposure time was 20 minutes, yielding an S/N ratio of 138 (Boesgaard & King 2002).

Table 1 gives a list of the stars observed for this program by HIP number and by HD number. The V magnitude, the UT date of the observation, the exposure time in minutes, and the

resulting S/N of the reduced spectrum near the Be II lines are listed. We have used the stellar parameters from the uniform set presented by Ramirez et al. (2012). Table 2 gives our sample of 1 $M_\odot$ stars with their values for temperature ($T_{\rm eff}$), log g, [Fe/ H], microturbulent velocity, ξ (calculated from the equation of Edvardsson et al. 1993), the Li abundance, A(Li) = log N(Li)/ log N(H) + 12.00, stellar mass, and age.

Figure 1 shows the distribution of the stars in Table 2 with $T_{\rm eff}$ and log g along with a zero-age main sequence. This shows that our stars are somewhat evolved off the main sequence making their ages more reliable as discussed by Ramirez et al. (2012). (One star, HIP 394, a subgiant with log g = 3.76 is not plotted.) The closest matches to the Sun are indicated with red dots; see discussion in Section 4.

Figure 2 plots the values for A(Li) in our Be sample as functions of temperature, mass, and age. (Again HIP 394 is not included.) The position of the Sun is given with the value of 0.96 ± 0.06 by Asplund et al. (2021). The range in stellar parameters of our observed stars is very narrow, but the Li abundances spread over 3 orders of magnitude. For the sample of stars we have observed, the position of the solar Li is in the lower third of all of those parameters for stars in its cohort.

3. Analysis

We have used the set of consistently determined stellar parameters of Ramirez et al. (2012) that are given in Table 2 to find Be abundances with our Keck/HIRES spectra. In order to
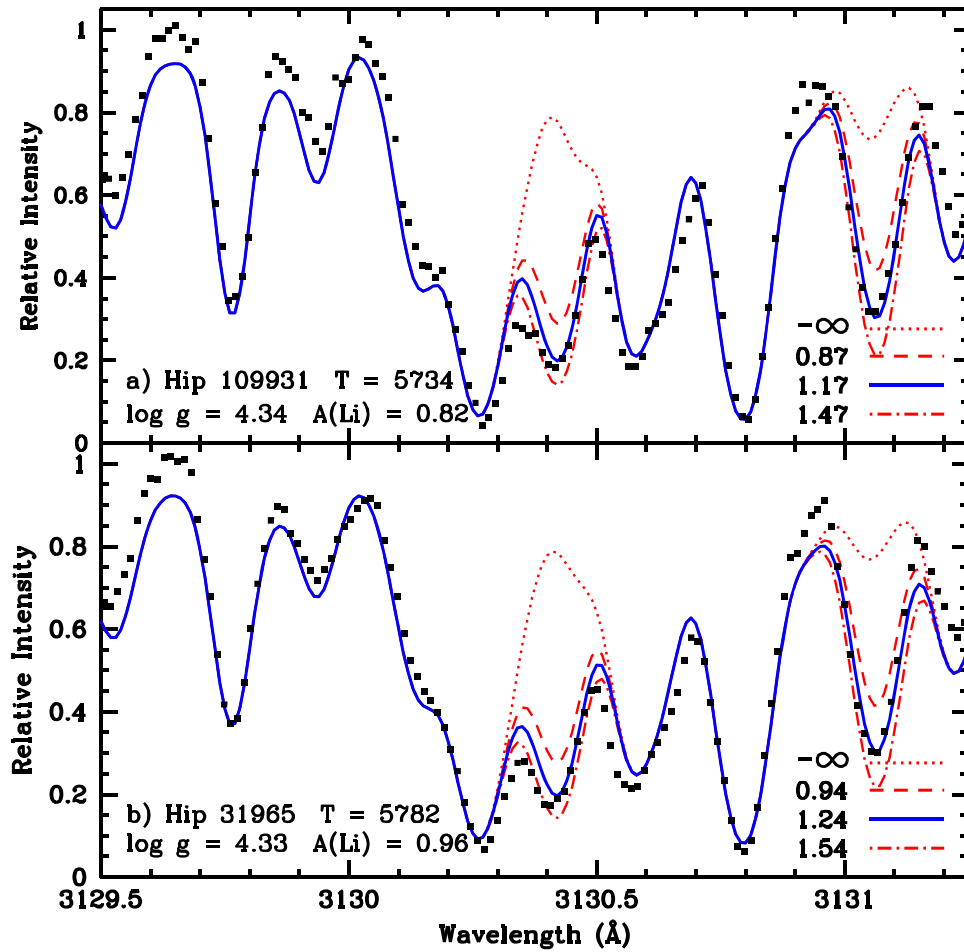

Figure 3. Spectrum syntheses in the Be II region for two of our stars. This shows 1.75 Å of the 3 Å region that we synthesized. The observed spectra are represented by the black squares. The best-fit synthesis is the solid blue line. A factor of 2 more Be is the red dashed–dotted line, a factor of 2 less Be is the red short dashed line, and a fit with no Be is the red dotted line.

determine the Be abundances, we have used the spectrum analysis program MOOG[8] (Sneden 1973; Sneden et al. 2012) as updated. The spectral region is so full of atomic and molecular lines that the method of spectrum synthesis must be used. We have analyzed our Keck/HIRES spectrum of the sky in the same way.

Examples of the synthesis fits for two of our stars are shown in Figure 3 along with a synthetic spectrum with no Be at all and one with 2 times more Be and with 2 times less. Table 3 gives the Be abundances as A(Be) for all 53 stars along with their temperatures and Li abundances as A(Li). Our value for A(Be) for the Sun is 1.23.

During the course of the synthesis process, we found two pairs of stars with virtually identical stellar parameters, but with very different Be contents. Figure 4 shows the Be II region of the normal Be star, HIP 1813 with A(Be) = 1.01, with that of HIP 32673 whose spectrum is virtually identical in every feature except the two Be II lines. The stars differ in temperature by 20 K, in log g by 0.14, and in [Fe/H] by 0.06. The mass difference is 0.01 and the ages are similar. Both are deficient in Li with upper limits on A(Li) of <1.08. Takeda et al. (2011) also found no evidence for Be in HIP 32673, listing A(Be) as <−0.78 and A(Li) as <1.04.

Figure 5 shows another pair of otherwise identical stars yet one has virtually no Be: HIP 58576 with normal Be at A(Be) = 1.21 and HIP 55846 with no Be. Those two stars are within 35 K in temperature, within 0.06 in log g, and within 0.01 in [Fe/H]. The Li abundance in the Be normal star (HIP 58576) is given as A(Li) = 0.32, with no upper limit sign; for HIP 55846, with undetectable Be, A(Li) is listed as 0.96, again, not listed as an upper limit (Ramirez et al. 2012).

The properties of these two pairs of stars along with their Li and Be abundances are shown in Table 4.

These two stars, HIP 32673 and HIP 55847, with no apparent Be II lines do show evidence of the presence of lines that blend with that Be II line. That spectral feature is due to a blend of Mn II at 3131.015, Mn I at 3131.037, and Fe I at 3131.043 Å. Those lines are included in our synthesis list.

3.1. NLTE Discussion

Calculations have been made of nonlocal thermodynamical effects (nLTE) on the Be abundance. A complete analysis was done by Chmielewski et al. (1975) of those effects in the solar spectrum. They found that Be is more ionized than expected in LTE and that the metastable level, $2p^3P^0$, of Be I is underpopulated. They calculated that the effects in the Sun were ≤0.10 dex. Those effects, caused by a hot radiation field in the uv, had been found to cancel out for Be by

---

Table 3
Lithium and Beryllium Abundances

HIP	$T_{\rm eff}$ (K)	A(Li)	A(Be)
394	5636	1.98	0.79
493	5943	2.31	1.00
996	5817	1.45	1.27
1411	5788	1.27	1.22
1813	5756	<1.08	1.01
7244	5767	2.26	1.22
7245	5801	1.82	1.09
23627	5791	1.57	1.10
24813	5860	2.03	1.35
25002	5741	2.36	0.96
25052	5749	<0.34	1.27
25414	5647	<1.13	1.21
30860	5527	<0.14	1.16
31965	5782	0.96	1.24
32673	5736	<1.07	<0.0
35599	5820	1.63	1.17
41184	5717	2.85	1.39
42438	5876	2.94	...
42723	6018	2.52	1.19
44935	5759	<0.88	1.09
49580	5794	1.95	1.09
50473	5925	2.20	1.14
52153	5791	1.91	1.27
54196	5877	2.51	1.12
54582	5826	1.56	0.99
55846	5463	<0.96	<0.0
56572	5511	<0.37	1.16
57300	6064	2.42	1.05
58576	5508	0.32	1.21
62039	5658	0.72	1.39
62198	5712	1.05	1.27
63354	6066	2.55	1.02
65049	5539	<0.66	1.28
65708	5735	0.69	1.20
72567	5942	2.86	1.04
73146	5731	1.22	1.34
100017	5902	2.22	1.10
100963	5786	1.63	1.10
100970	5733	1.29	1.37
104075	5893	2.71	1.11
106678	5644	0.42	1.21
107350	5942	2.93	1.00
108468	5799	<1.03	1.16
109090	5993	2.41	1.09
109110	5815	2.45	1.09
109378	5526	<0.41	1.22
109931	5734	0.82	1.17
110035	5830	1.65	1.17
112504	5753	1.97	1.17
115370	5896	1.85	1.10
116906	5744	1.08	1.09
118115	5836	<1.11	1.20
118159	5848	2.71	1.16

Kiselman & Carlsson (1995) and to be less than 0.10 dex. These nLTE investigations were extended to more metal-poor stars by Garcia Lopez et al. (1995). They also conclude that the effects are <0.10. Additional discussion about nLTE effects can be found in the review article by Asplund (2005).

Very recently, Korotin & Kucinskas (2022) used new atomic data and calculated and tabulated the corrections for nLTE effects on Be for four values of [Fe/H]: -2.0, -1.0, 0.0, and $+0.5$ for three values of [Be/Fe]: -0.5, 0.0 $+0.5$. Their

calculations cover six temperatures from 4500–6500 K and seven values of log g from 0.0 to 5.0. For stars with our solar parameters, the effects are small, e.g., at $T = 6000$ K, log $g = 4.5$, and [Fe/H] = 0.0, the correction is -0.06 dex. We have not applied this correction to our results.

3.2. Error Discussion

Ramirez et al. (2012) list the errors in the stellar parameters for all 1381 stars in their Li abundance study. In turn, we have examined those errors in $T_{\rm eff}$, log g, and [Fe/H] in our subset of those stars. Virtually all show ± 50 K in temperature and ± 0.04 in [Fe/H] with a range of ± 0.03 to ± 0.08 in log g. In all of our Be analyses we have evaluated Be errors in grid model atmospheres for two values of Be line blends for four temperatures (5750, 6000, 6250, and 6500 K), three log g values (4.5, 4.0, and 3.5), three metallicities ([Fe/H] = -0.1, 0.00, and $+0.1$) and two microturbulent velocities (1.25 and 1.5 km s^{-1}). From that, we can assess the errors in the Be abundances, which are due to the choice of those stellar parameters. For example, for an error in log g of 0.5, the error in A(Be) was found to be ± 0.25. For our stars, the typical error in log g from Ramirez et al. (2012) is 0.05 so that would result in an error in A(Be) of ± 0.025. An uncertainty of ± 50 K in temperature results in an uncertainty of <0.01 in A(Be). The uncertainty of 0.05 in [Fe/H] gives a Be abundance uncertainty of ± 0.02.

The uncertainty in A(Be) does not only result from the errors associated with the stellar parameters. The ultraviolet spectral region where the Be II resonance lines are located is very crowded with atomic and molecular lines. The identification of these lines, as well as information on the excitation potentials and especially the transition probabilities, is input into the abundance determination. The list of blending lines, their wavelengths, and their atomic characteristics can be another potential source of error even though those are well known for the two Be II lines.

The model atmosphere and the line list provide calculated spectra; the process of matching that with the observed has a subjective element. This introduces another uncertainty into the final value of the Be abundance, which is difficult to quantify. Overall, we suggest that the typical error in A(Be) is ± 0.12.

We have results for nine stars to compare with those of Takeda et al. (2011) so we can compare our parameters and abundances of Li and Be with their values. There is a systematic difference in that all our Be abundances are lower than theirs with a range of -0.01 to -0.35 and a mean difference of -0.17 ± 0.12. Our temperatures are in good agreement; on average, ours are $\sim 12°$ K hotter. Our values for log g are within ± 0.03 on average. We suspect the Be differences are therefore contained in the line list parameters we use in our respective syntheses. In the region between 3129.0 and 3132.9 Å, our list does contain 171 lines compared to theirs of 124 or 47 more lines than their list. Many weak lines would tend to depress the continuum in the calculated spectrum and lower the Be abundance.

4. Results

Our final results for A(Be) are given in Table 3 along with the values for A(Li) from Ramirez et al. (2012) for 53 stars. The upper limits on the values we found for Be in two stars and those reported by Ramirez et al. (2012) for Li in 12 stars are
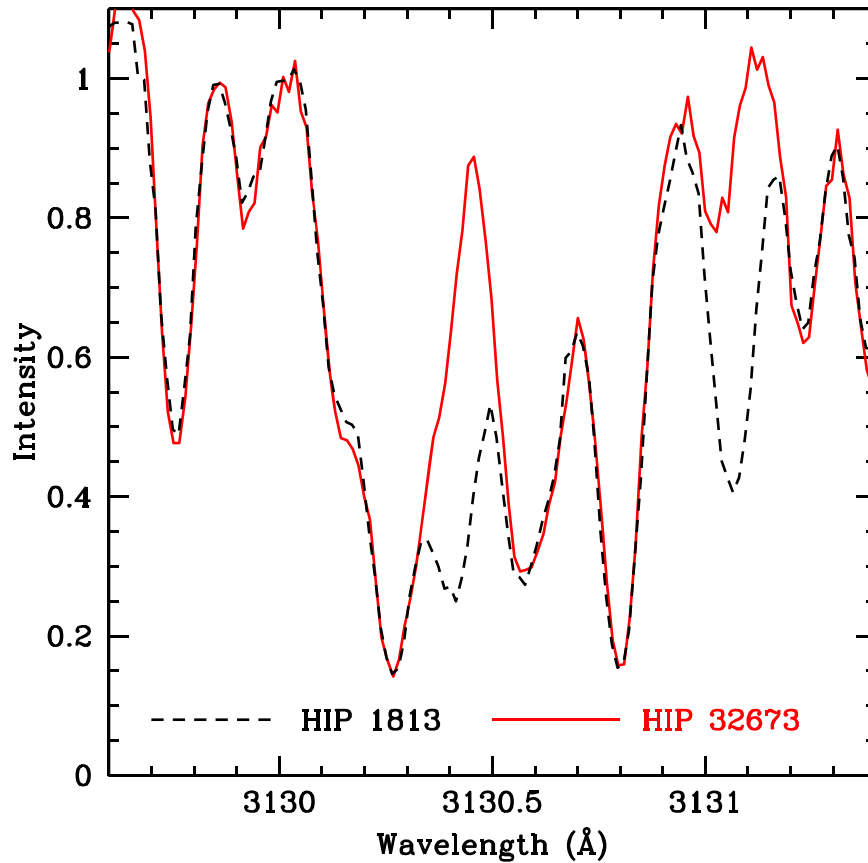
Boesgaard et al.

Figure 4. Spectra in the Be II region of two similar stars with very different Be content. HIP 32673, shown as the solid red line, appears to have no Be present in either of the two Be II lines. HIP 1813, shown by the dashed black line, has A(Be) = 1.01. The temperature for the Be-less star is 5736 K and that of HIP 1813 is 5756 K. Their values of [Fe/H] are solar at 0.03 and −0.03 for HIP 32673 and HIP 1813, respectively, and their ages are 6.61 and 7.95 respectively.

indicated by "<" signs. (Although we observed and analyzed HIP 394, we have not included it in any of the figures because it is a subgiant and out of our range in mass and metallicity.)

In Figure 6 we show our results for the Be abundances with mass (left) and with temperature (right). The horizontal line in each graph represents the solar Be abundance at A(Be) = 1.23 derived from our Keck/HIRES sky spectrum. The solar-mass value is indicated by the vertical line and the solar temperature of 5772 K is the vertical line in that plot. The error bar for A(Be), ±0.12, is shown in the lower left for each graph. The spread in A(Be) is larger than a typical 1σ error bar but within 3σ. About 80% of our sample is within 2% of the solar mass with a mean value of A(Be) of ∼1.2. There is no theoretical expectation of any trend of A(Be) with temperature.

Figure 7 shows our Be results with [Fe/H] (left) and with stellar age (right). There is a trend of A(Be) with [Fe/H] in this small range in [Fe/H]. This is similar to that found by Boesgaard et al. (2004) for 20 solar-like stars with temperatures spanning 5618–6718 K and metallicities from [Fe/H] of −0.52 to +0.11 all having undepleted Be abundances; that measured slope is 0.38 ±0.14. Our larger sample of 52 stars here gives a slope of 0.34 ±0.09, which is shown in Figure 7, left. It is possible to see a small increase in A(Be) with stellar age, Figure 7, right. These would be expected from slow Galactic production of the rare light elements by cosmic-ray spallation and novae.

One curious result is the identification of two pairs of stars with virtually identical parameters, but one star in each pair has no detectable Be. These pairs were shown above in Figures 4

and 5. We note that Takeda et al. (2011) reported four stars with low Be including HIP 32673. The two stars with little or no Be, HIP 32673 and 55846, may well have lost their Be and Li through mass transfer or a stellar merger with a companion, akin to those discussed by Boesgaard (2007). In that work the lack of Li and Be in a few metal-poor halo stars was attributed to the destruction of Li and Be by thorough and deep mixing in close binaries or merging pairs. We note that HIP 55846 is a binary star, 83 Leo. This mass-transfer activity may also account for the other three stars reported by Takeda et al. (2011) to have no Be.

In Figures 7 and 8, we have shown our results for Be with our value for solar Be from our Keck spectrum with a horizontal dotted line at A(Be) = 1.23. Now we can put our values for Li and Be on the same abundance scale and normalize them to a common maximum: A(Li) = 3.27 (Lodders 2021) and A(Be) = 1.38 (Asplund et al. 2021). These results are shown in Figures 8–11 for mass, temperature, metallicity, and age. In each of these figures, our value for solar Be at 1.23 is shown by the large yellow disk inside the blue circle and the solar value for Li of 0.96 is the large yellow disk inside the red circle. In these 1 $M_\odot$ stars, the Li abundances range over 3 orders of magnitude while the Be abundances cover a span of little more than a factor of 2.5 (with the exception of the two stars with only upper limits on the Be abundance).

Although we have used the solar Be abundance, A(Be) = 1.38 from Asplund et al. (2021) to scale our results, this value for the Sun is not certain. Those authors note in their discussion of Be that this number could be too high due to
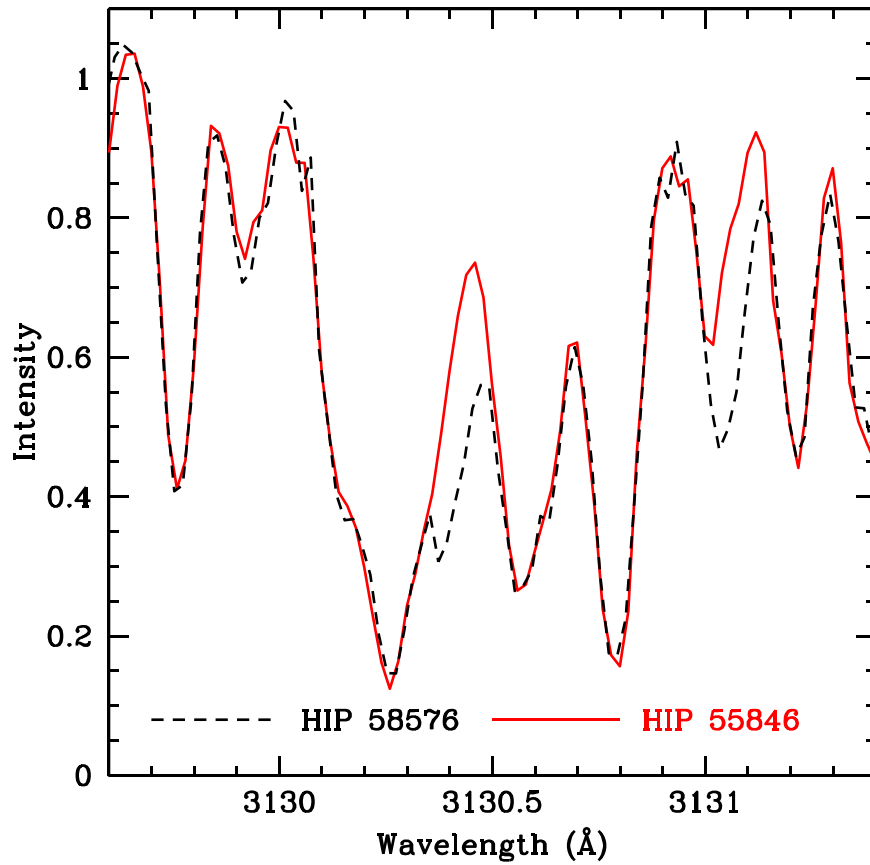
Figure 5. Spectra in the Be II region of two similar stars with very different Be content. HIP 55846, solid red line, appears to have no Be present in either of the two Be II lines. The black dashed line shows the Be region of HIP 58576 with A(Be) = 1.21. As in the previous figure, these two stars are similar in other respects: HIP 55846, with no Be, has T = 5463 K, [Fe/H] = 0.30, and age = 3.45 Gyr, while HIP 58576, dashed black line, has T = 5508 K, [Fe/H = 0.31, and age = 6.71 Gyr.

Table 4
Two Stars with No Beryllium with Matching Twins with Beryllium

HIP	T_{eff}(K)	log g	[Fe/H]	Mass	Age (Gyr)	A(Li)	A(Be)
1813	5756	4.30	−0.03	0.98	7.95	<1.08	1.01
32673	5736	4.44	+0.03	0.99	6.61	<1.07	<0.0
58576	5508	4.42	+0.31	1.00	6.71	0.32	1.21
55846	5463	4.48	+0.30	0.99	3.45	0.96	<0.0

blending features that may not have been included. Our Keck daytime sky spectrum yields solar A(Be) = 1.23. As mentioned at the end of Section 3.2, many weak lines would depress the continuum and thus lower the Be abundance.

We note that Takeda et al. (2011) found 1.22 for solar Be. In their careful and detailed new study of solar Be, Carlberg et al. (2018) found 1.30 from a spectrum of the asteroid Vesta. Our subset of the 10 stars that are most similar to the Sun in all five parameters (see Table 5) has a mean value of A(Be) = 1.18 with a range of 1.09–1.27. Figure 8 shows the distribution of Li and Be abundances with stellar mass. The spread in Li is seen clearly and is particularly true within the narrower mass span of 0.98–1.02 $M_\odot$. This figure also highlights the small range of masses in our sample.

The spread in Li abundance with the stellar surface temperature is shown in Figure 9. This figure reveals a trend of A(Li) with T_{eff} with more Li depletion at cooler temperatures with a steep decline from 6000 to 5700 K. Inasmuch as Be

must be mixed deeper to higher temperatures to be destroyed, there is no such trend seen in the Be abundances.

Figure 10 shows the relationship between stellar metallicity and Be abundance seen in Figure 7 (left) with a slope of 0.34 ±0.09. There is a broad decline in Li with [Fe/H] due to Li depletion. Although the range in [Fe/H] is relatively small, a factor of 6, some of the spread may come from the reduced opacity in the lower-metallicity stars, causing reduced mixing and greater Li retention. There may be a discernible relation between Be and metallicity as discussed in Figure 7, left.

Our subset of 1 $M_\odot$ stars has had age determinations made by Ramirez et al. (2012) with isochrones. (They give error bars that indicate a sizable range, with some of the older stars perhaps 2–3 Gyr.) Figure 11 shows the Li and Be abundances with stellar age. There is a spread in Li at most ages but small Li depletions at the youngest ages. A trend of increasing Be with age can be discerned as shown in Figure 7, right.

We have confined our already restricted sample to the stars that are the most similar to the Sun in the five properties of mass, temperature, metallicity, surface gravity, and age. Those stars and the Sun are given in Table 5 along with their defining characteristics. The high and low values for mass, T_{eff}, log g, [Fe/H], age, and A(Be) are given with the mean values and probable errors of those means for the 10 stars. The range in A(Be) is 1.09–1.27 with a mean of 1.18; however, the spread in A(Li) is much larger: 0.82–2.71.

The value of the solar Li is in the lower third of our total sample of solar-mass stars. In our sample of the 10 closest
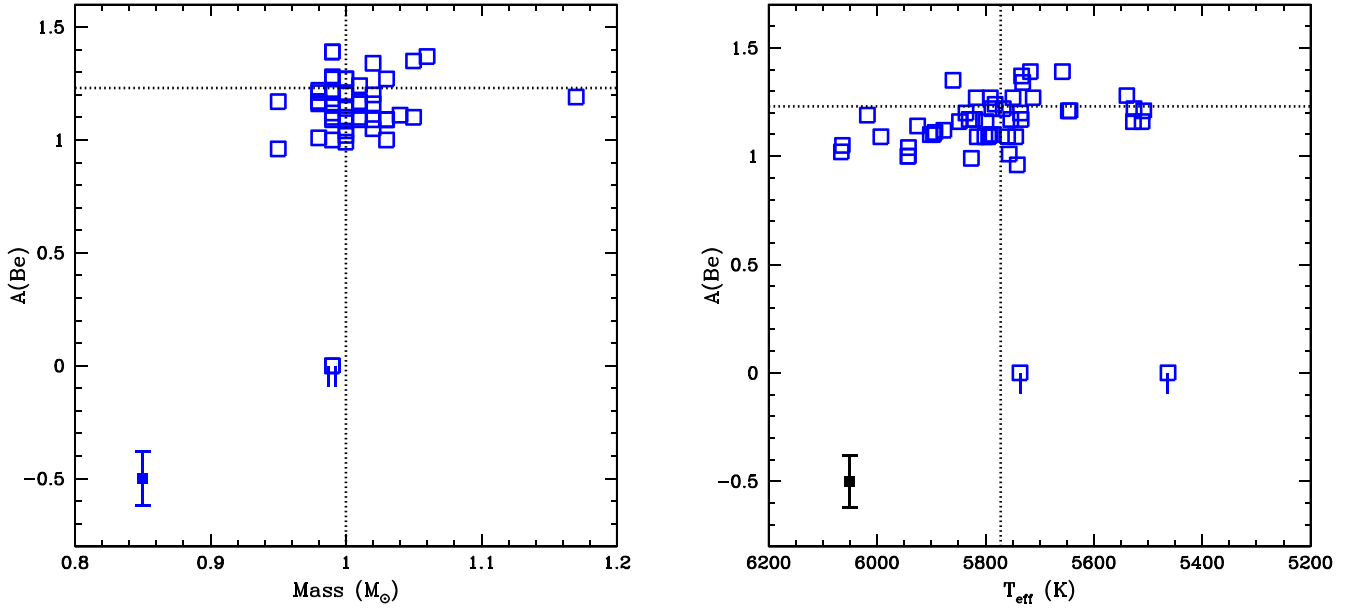
Figure 6. Left: beryllium abundances, A(Be), as a function of stellar mass shown as open blue squares. Right: beryllium abundances, A(Be), as a function of surface temperature. For each figure, the short vertical blue lines attached to two of the open squares indicate upper limits on the Be abundance. The horizontal dotted line represents the solar Be abundance at A(Be) = 1.23 from our Keck/HIRES sky spectrum. The vertical blue dotted lines indicate the solar mass and temperature, respectively. A typical error bar is shown in the lower left.
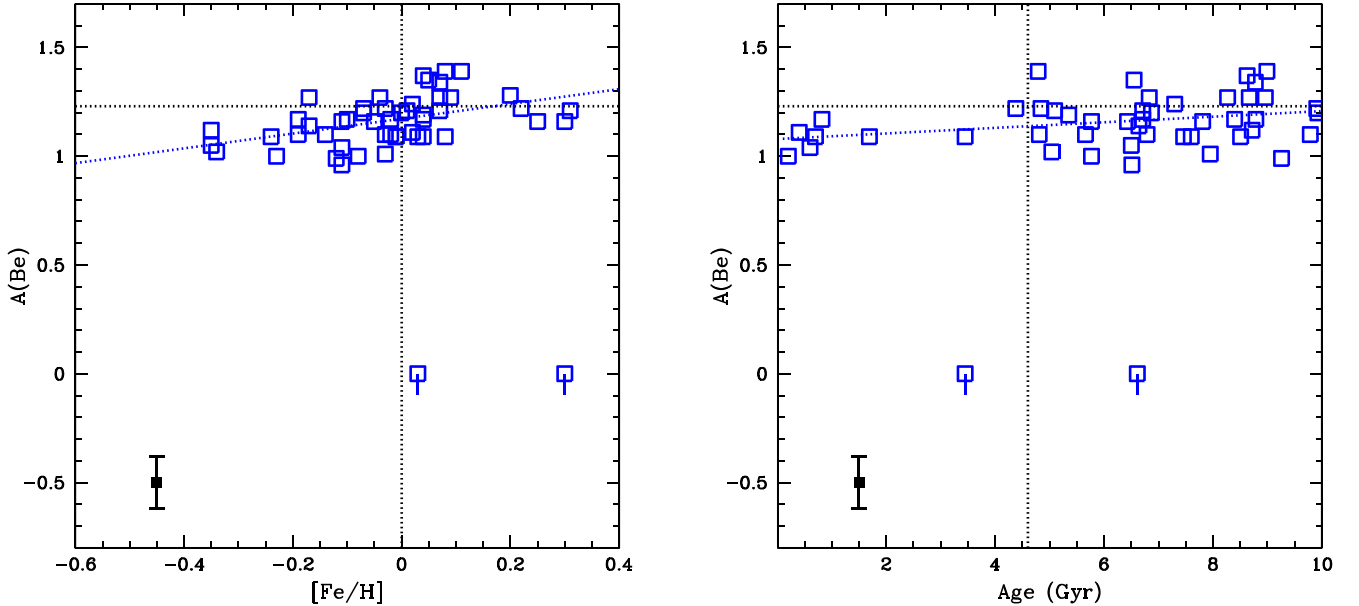
Figure 7. Left: beryllium abundances, A(Be), as a function of [Fe/H] shown as an open blue square. The blue dotted line through the points is a least-squares fit with a slope of 0.34 ± 0.09. Right: beryllium abundances, A(Be), as a function of age. The blue dotted line is a least-squares fit through the points and has a slope of 0.013 ± 0.005. For both figures, the vertical blue lines attached to two points indicate upper limits on the Be abundance and were not included in the fit. The horizontal dotted line represents the solar Be abundance at A(Be) = 1.23 in our Keck/HIRES sky spectrum. The vertical dotted line represents the solar mass and temperature, respectively. A typical error bar is shown in the lower left.

clones of the Sun; however, there is only one star with less Li than the Sun, HIP 109931, at A(Li) = 0.82. The Sun seems exceptionally depleted in Li. However, it is among the upper third in its Be content.

Rotational models of light element depletion (e.g., Deliyannis & Pinsonneault 1997) show a slope between A(Be) and A(Li) of about 0.4 in F dwarfs in close agreement with observations (Deliyannis et al. (1998). The model slope decreases with cooler stars as the deeper convection zones play a greater role in depleting Li but not Be. We have a

subsample of 29 stars between ± 100 K of the solar value of 5772 K. The range of Li/Be is 0.31–35.5. Figure 12, left, shows the plot of A(Li) with A(Be) for those stars showing a slope of -0.008, virtually no slope. A cleaner subsample is the stars given in Table 5, which are the 10 most similar to the Sun in all five parameters. There are no stars with upper limits on A(Li) in that sample. For those stars, the Li/Be range is 0.45–35.5. The plot for those stars is shown in Figure 12, right. That slope is also negligible at -0.022. The Deliyannis & Pinsonneault (1997) models suggest a slope of 0.2 at 1 $M_\odot$, so
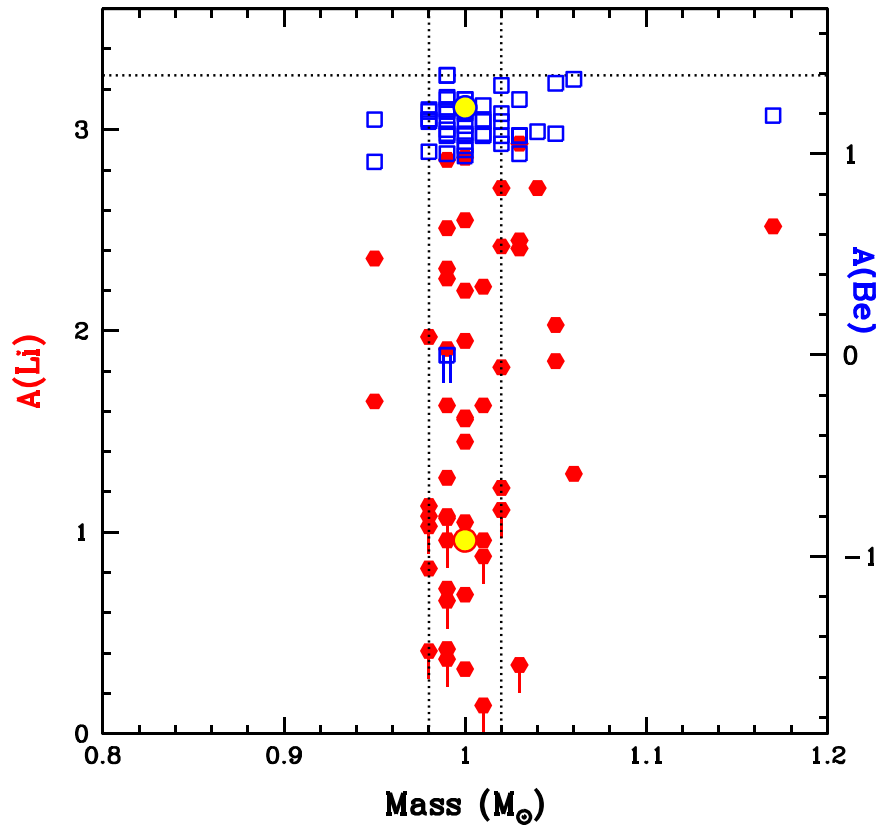
Figure 8. Abundances of Li and Be as a function of stellar mass. The abundances of the two elements are on the same scale, normalized to their respective undepleted abundances: $A(Li) = 3.27$ from meteorites (Lodders 2021) and $A(Be) = 1.38$ for the Sun (Asplund et al. 2021). The values for $A(Li)$ are red hexagons and for $A(Be)$ are blue open squares. The upper limits on the abundances of both elements are indicated by a vertical line beneath the plotted points. The solar $A(Li)$ from Asplund et al. (2021) of 0.96 is shown as a filled yellow ball surrounded by a red circle. Our solar $A(Be)$ value of 1.23 is a yellow ball surrounded by a blue circle. Whereas the Li points show a large spread over this small range of stellar mass, the Be points are clustered together, with the exception of the two stars with no apparent Be. The two vertical dotted lines delineate the 0.98 and 1.02 solar masses.

either the models deplete too much Be or other mechanisms contribute to the mixing. Models show that gravity waves affect Li more than Be (e.g., Garcia Lopez & Spruit 1991).

5. Summary and Conclusions

We have made observations of the resonance lines of Be II in 53 main-sequence stars within approximately $\pm 0.02\,M_\odot$ at high spectral resolution (45,000) and high S/N ($\sim$50–180) with the upgraded HIRES on the Keck I telescope. These observations took place over the course of four observing runs between 2014 and 2019. Our sample comes from stars with known Li abundances and stellar parameters determined in a uniform way for 1581 stars by Ramirez et al. (2012). With those parameters, we have found Be abundances, $A(Be)$, through spectrum synthesis with an advanced version of MOOG.

We have found two pairs of virtually identical stars in their parameters and spectra, except one of each pair has normal Be and the other has no evidence of either Be II line. We suggest that the stars with no Be, HIP 32673 and 55846, have undergone a mass-exchange event or a merger with a companion that has thoroughly redistributed matter such that the Li and Be material has been destroyed at high temperatures by thermonuclear reactions.

When we exclude the two stars with no visible Be features, we find that our solar-mass stars have very similar Be abundances. With the exception of the subgiant star, HIP

394, the spread in $A(Be)$ is 0.96 to $1.39 = 0.43$, corresponding to a factor of 2.7 for these G dwarfs. We estimate the error in the determination of $A(Be)$ to be ± 0.12.

For this set of stars, the range in $A(Li)$ found by Ramirez et al. (2012) is <0.14 to 2.94 or 2.80, corresponding to over 630 times. Considering only the stars with detectable Li, the range is 2.62 or a factor of more than 400.

Standard Li depletions corresponding to our solar-mass stars occur only during the pre-main-sequence evolution (Deliyannis et al. 1990; Pinsonneault 1997) when the stars are cooler and are fully convective. Observations of the young Pleiades show no Li depletion among the F and G dwarfs (Pilachowski et al. 1987; Boesgaard et al. 1988). This is matched by calculations of the Li–temperature relation for slowly rotating young stars (Somers & Pinsonneault 2014). However, Li abundances in main-sequence stars in older open clusters indicate that Li depletion continues during the main-sequence phase. Consistent with this, our entire sample lies below the Pleiades Li value of $A(Li) \geqslant 3.0$. This requires an additional mixing mechanism(s), and rotational mixing is a prime candidate (Deliyannis & Pinsonneault 1997; Somers & Pinsonneault 2014).

We have shown our Be abundance results as a function of mass and temperature in Figure 6 and as a function of metallicity and age in Figure 7. There is a linear relationship showing that $A(Be)$ increases with [Fe/H] and with age, which would be expected from Galactic enrichment of the rare light
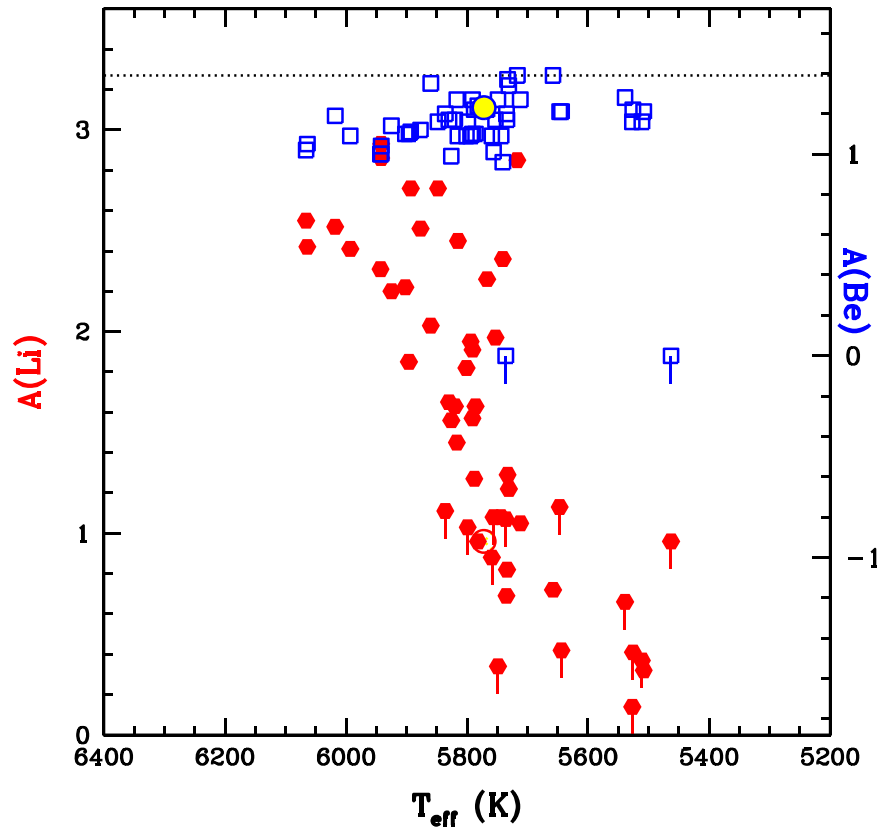
Figure 9. Abundances of Li and Be as a function of surface temperature, on the same scale and normalized as in the previous figure. The symbols and upper limits are as in the previous figure as are the solar symbols. The Li results show a large spread with a trend toward lower Li with lower temperature. The Be results show a minimal spread with two stars having only upper limits.
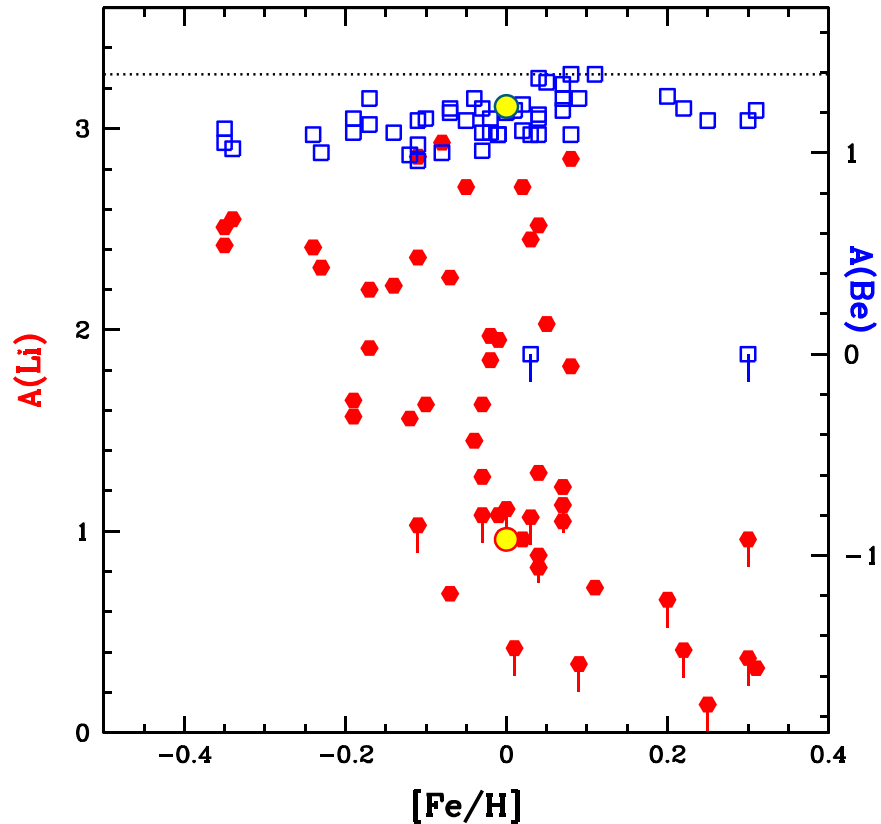

Figure 10. Abundances of Li and Be as a function of Fe abundance, again normalized and scaled as in Figure 8. The symbols and upper limits are as in the previous figures as are the solar symbols. There is a general broad decline in Li with declining metallicity. For Be, there is a mild increase due to a general Galactic production of light elements.
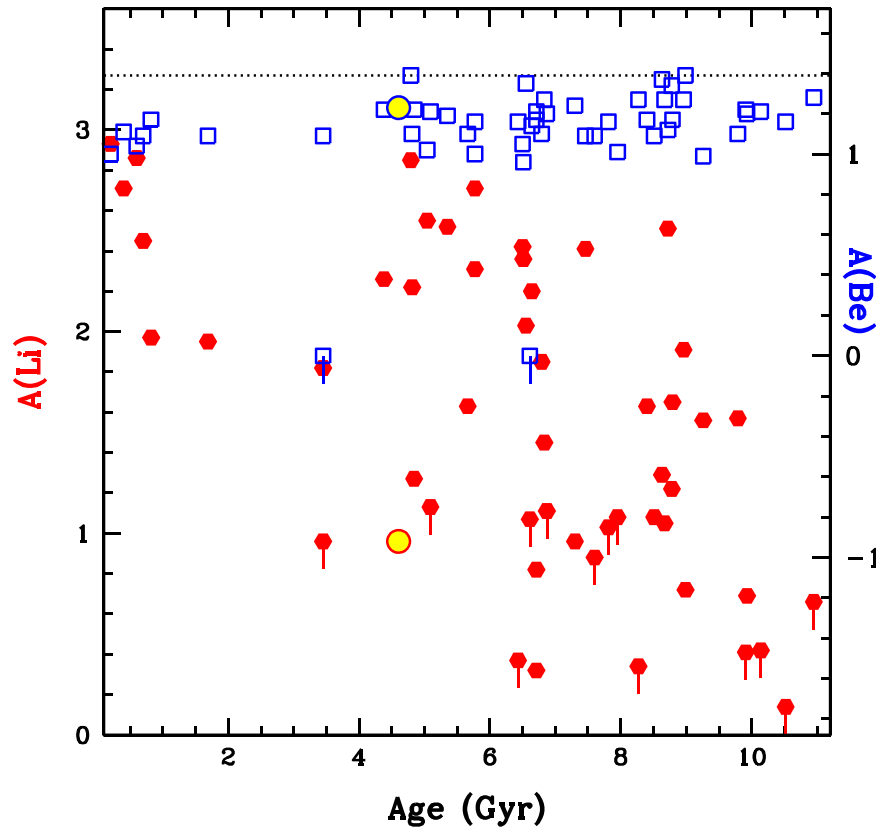
Figure 11. Abundances of Li and Be as a function of age, again normalized and scaled. The symbols and upper limits are as in the previous figures as are the solar symbols. The values of $A(Be)$ show a mild increase with age. For Li, there is a wide spread with age and little noticeable trend with age.

Table 5
Close Solar Twins

HIP	Mass	T_{eff} (K)	log g	[Fe/H]	Age (Gyr)	$A(Li)$	$A(Be)$
996	1.00	5817	4.32	−0.04	6.83	1.45	1.27
1411	0.99	5788	4.35	−0.03	4.84	1.27	1.22
7244	0.99	5767	4.46	−0.07	4.38	2.26	1.22
7245	1.02	5801	4.42	+0.08	3.45	1.82	1.09
31965	1.01	5782	4.33	+0.02	7.30	0.96	1.24
62198	1.00	5712	4.34	+0.07	8.67	1.05	1.27
100963	0.99	5786	4.44	−0.03	5.66	1.63	1.10
109931	0.98	5734	4.34	+0.04	6.71	0.82	1.17
116906	0.99	5744	4.31	−0.01	8.51	1.08	1.09
118159	1.02	5848	4.42	−0.05	5.77	2.71	1.16
Sun/sky	1.00	5772	4.44	0.00	4.603	0.96	1.23
low	0.98	5712	4.31	−0.07	3.45	0.82	1.09
high	1.02	5848	4.46	0.08	8.67	2.71	1.27
means	1.00	5778	4.37	−0.002	6.21	⋯	1.18
p.e.	±0.01	±40	±0.05	±0.005	±1.72	⋯	±0.07

elements given no stellar depletion losses; such depletion is not expected for Be in solar-mass stars.

The large range in Li compared to the narrow range in Be can be seen especially clearly in our Figure 8, where those abundances are displayed with stellar mass. The abundance results are plotted on the same scale and adjusted to their respective solar/solar system values. In stellar mass, most of our sample of stars is between 0.98 and 1.02 $M_\odot$.

In the narrow range of mass, 0.98–1.02, we find a small dispersion in $A(Be)$ with a range from 0.99 to 1.39. However,

Ramirez et al. (2012) found the spread in $A(Li)$ in these stars covered 0.32–2.94 as shown in Figure 8.

Figure 9 shows a steep decline of $A(Li)$ with T_{eff} such that the cooler stars show greater amounts of Li depletion than the warmer ones. The surface amount of Be seems unaffected in these stars. There is a considerable spread in the Li abundances at any temperature. Some may be intrinsic spread and errors, but some can be attributed to age and metallicity differences and some may be inherent in the depletion mechanisms. The limits we can place on Be depletion provide more constraints.
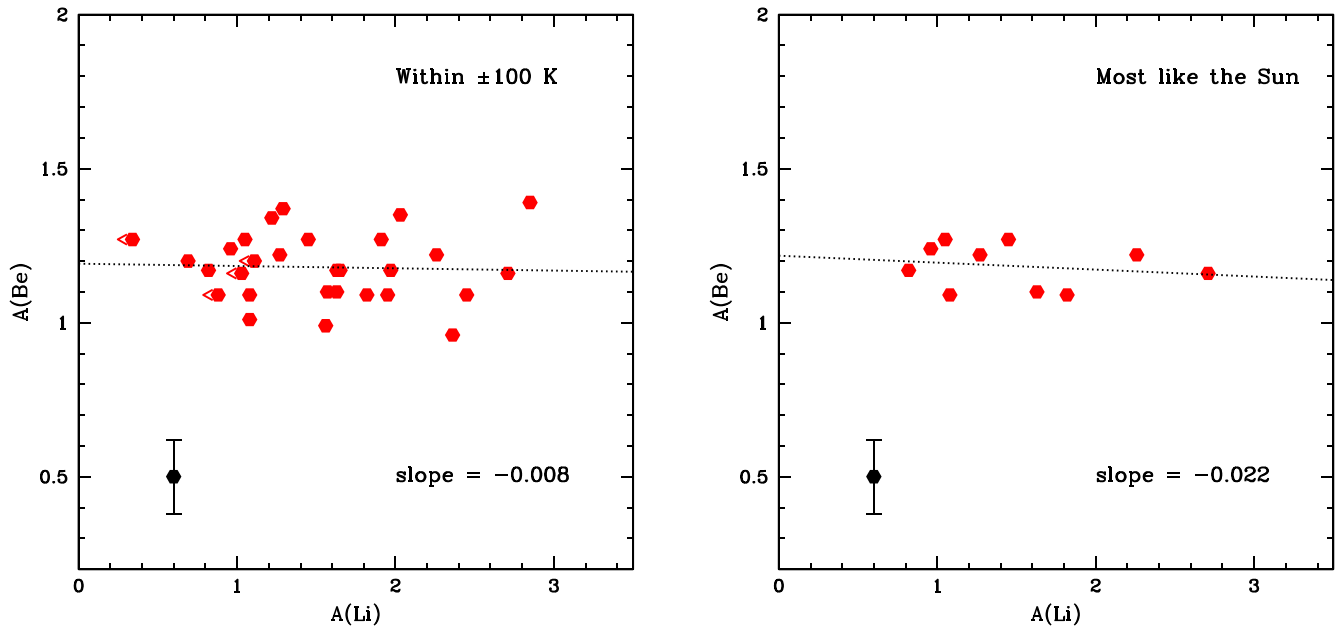
Figure 12. Left: lithium abundance versus beryllium abundance for a sample of stars within ±100 K of the solar temperature. Upper limits on A(Li) are shown with <. There is no discernible slope. Right: Li and Be abundances for the 10 stars most similar to the Sun from Table 5. Again the slope is negligible.

The rotational mixing models of Deliyannis & Pinsonneault (1990) deplete Be by as much as 0.4 dex. The total range for our solar-mass stars is 0.4 dex; some may be beyond the errors and be intrinsic. If our errors are 0.12 dex, then any intrinsic scatter must be smaller. This limit also constrains the efficiency of mixing below the surface convection zone and may allow mixing by gravity waves to play a role. Compared to models with rotational mixing, models with mixing due to gravity waves affect Li more than Be.

There is a trend of A(Be) with [Fe/H] as seen in Figure 7 (left) and Figure 10. For our 52 stars with [Fe/H] between −0.4 and +0.4, we have found a slope of 0.34 ± 0.09. This is a good indicator of the gradual production of the light elements during Galactic evolution by cosmic-ray spallation and in novae. Such a trend cannot be delineated well with Li as it is so readily depleted by stars. This effect in Be with stellar age is seen also, but ages are not as well determined as [Fe/H] values. There is a large spread in Li over the 11 Gyr age range of our stars revealed in Figure 11.

We have looked at the 10 stars most similar to the Sun in all five parameters: mass, metallicity, age, effective temperature, and surface gravity. For those 10 stars, we have found that the range in A(Li) is 0.82–2.71, a factor of 80, while the range in A(Be) is only 1.09–1.27, a factor of 1.5. The Li/Be ratio spans 0.45 to 35, almost 2 orders of magnitude, due to the range in Li abundance. Figure 12 shows there is no trend between Li and Be abundances in that subsample nor in the sample of 29 stars within ±100 K of the solar temperature. This result suggests that additional mechanisms may contribute to the mixing of Li below the convection zone.

Our selection of stars from a large and uniform collection of FGK stars observed for Li provides a means to investigate an aspect of stellar interiors and evolution. The inclusion of Be abundances gives additional depth to the investigation.

We wish to express our appreciation for their knowledgeable help during our observing runs to the Keck Observatory support astronomers and staff. A.C. acknowledges her graduate

ORCID iDs

Ann Merchant Boesgaard https://orcid.org/0000-0002-8468-9532
Constantine P. Deliyannis https://orcid.org/0000-0002-3854-050X
Michael G. Lum https://orcid.org/0000-0001-7205-1593
Ashley Chontos https://orcid.org/0000-0003-1125-2564

References

Anders, E., & Grevesse, N. 1989, GeCoA, 53, 197
Asplund, M. 2005, ARA&A, 43, 481
Asplund, M., Amarsi, A. M., & Grevesse, N. 2021, A&A, 653, A141
Balachandran, S., & Bell, R. 1998, Natur, 392, 791
Boesgaard, A. M. 2007, ApJ, 667, 1196
Boesgaard, A. M., Budge, K. G., & Ramsey, M. E. 1988, ApJ, 327, 389
Boesgaard, A. M., & Hollek, J. K. 2009, ApJ, 691, 1412
Boesgaard, A. M., & King, J. R. 2002, ApJ, 565, 587
Boesgaard, A. M., Lum, M. G., & Deliyannis, C. P. 2020, ApJ, 888, 28
Boesgaard, A. M., McGrath, E. J., Lambert, D. L., & Cunha, K. 2004, ApJ, 606, 306
Boesgaard, A. M., Rich, J. A., Levesque, E. M., & Bower, B. P. 2011, ApJ, 743, 140
Carlberg, J., Cunha, K., Smith, V. V., et al. 2018, ApJ, 865, 8
Carlos, M., Melendez, J., Spina, L., et al. 2019, MNRAS, 485, 4052
Chmielewski, Y., Mueller, E. H., & Brault, J. W. 1975, A&A, 42, 37
Deliyannis, C. P., Boesgaard, A. M., Stephens, A., et al. 1998, ApJ, 498, 147
Deliyannis, C. P., Demarque, P., & Kawaler, S. D. 1990, ApJS, 73, 21
Deliyannis, C. P., & Pinsonneault, M. H. 1990, ApJS, 74, 501
Deliyannis, C. P., & Pinsonneault, M. H. 1997, ApJ, 488, 836
Demarque, P., Woo, J. H., Kim, Y.-C., & Yi, S. K. 2004, ApJS, 155, 677
Edvardsson, B., Andersen, J., Gustafsson, B., et al. 1993, A&A, 500, 391
Garcia Lopez, R. J., Severino, G., & Gomez, M. T. 1995, A&A, 297, 787
Garcia Lopez, R. J., & Spruit, H. 1991, ApJ, 377, 268
Greenstein, J. L., & Richardson, R. S. 1951, ApJ, 113, 536
Greenstein, J. L., & Tandberg Hansen, E. 1954, ApJ, 119, 113

Kiselman, D., & Carlsson, M. 1995, in The Light Element Abundances, ed. P. Crane (Berlin: Springer), 372
Korotin, S., & Kucinskas, A. 2022, A&A, 657, L11
Lodders, K. 2021, SSRv, 217, 44
Matsuno, T., Aoki, W., Suda, T., & Li, H. 2017, PASJ, 69, 24
Pilachowski, C. A., Booth, J., & Hobbs, L. M. 1987, PASP, 99, 1288
Pinsonneault, M. H. 1997, ARA&A, 35, 557
Ramirez, I., Fish, J. R., Lambert, D. L., & Allende Prieto, C. 2012, ApJ, 756, 46
Sneden, C. 1973, ApJ, 184, 839
Sneden, C., Bean, J., Ivans, I., et al. 2012, MOOG: LTE Line Analysis and Spectrum Synthesis, Astrophysics Source Code Library, ascl:1202.009
Somers, G., & Pinsonneault, M. H. 2014, ApJ, 790, 72
Somers, G., & Pinsonneault, M. H. 2016, ApJ, 829, 32
Takeda, Y., Tajitsu, A., Honda, S., et al. 2011, PASJ, 63, 697
Thevenin, F., Oreshina, A. ,V., Baturin, V. A., et al. 2017, A&A, 598, 64
Tody, D. 1986, Proc. SPIE, 627, 733
Tody, D. 1993, in ASP Conf. Ser. 52, Astronomical Data Analysis Software and Systems II, ed. R. J. Hanisch et al. (San Francisco, CA: ASP), 173
Vogt, S. S., Allen, S. L., Bigelow, B. C., et al. 1994, Proc. SPIE, 2198, 362